



## Caffeic acid oligomers from *Mesona chinensis* and their *In Vitro* antiviral activities



Zi-Qin Wang<sup>a,b,1</sup>, Qiao-Yun Song<sup>a,b,1</sup>, Jun-Cheng Su<sup>a,b</sup>, Wei Tang<sup>a,b</sup>, Jian-Guo Song<sup>a,b</sup>,  
Xiao-Jun Huang<sup>a,b</sup>, Jinmeng An<sup>c</sup>, Yao-Lan Li<sup>a,b</sup>, Wen-Cai Ye<sup>a,b,\*</sup>, Ying Wang<sup>a,b,\*</sup>

<sup>a</sup> Institute of Traditional Chinese Medicine & Natural Products, College of Pharmacy, Jinan University, Guangzhou 510632, People's Republic of China

<sup>b</sup> Guangdong Province Key Laboratory of Pharmacodynamic Constituents of TCM & New Drugs Research, Jinan University, Guangzhou 510632, People's Republic of China

<sup>c</sup> Guangzhou Wanglaoji Great Health Industry Co., Ltd., Guangzhou 510623, People's Republic of China

### ARTICLE INFO

#### Keywords:

*Mesona chinensis*  
Caffeic acid oligomer  
Anti-RSV activity

### ABSTRACT

The phytochemical study of the aerial part of *Mesona chinensis* led to the isolation of five new caffeic acid oligomers (1–5), as well as four known analogues (6–9). The structures of the new compounds including their absolute configurations were elucidated by comprehensive spectroscopic analysis, chemical method, and quantum-chemical electronic circular dichroism (ECD) calculation. Among the isolates, compound **7** showed significant *in vitro* antiviral activity on respiratory syncytial virus (RSV).

### 1. Introduction

The plant *Mesona chinensis* Benth. (Lamiaceae), commonly known as “jellywort”, is a yearly herbaceous plant that widely distributed in tropical and subtropical areas of Asia [1]. For hundreds of years, this plant was of particular interest by local people due to its economical and agricultural values for making grass jelly and herbal tea. Moreover, in the southern region of China, *M. chinensis* has been used as a Chinese folk medicine for the treatment of heat-shock, fever, hypertension, and inflammatory [2,3]. Previous chemical investigations of *M. chinensis* mainly focused on the bioactive polysaccharides [4–9], there are a few reports about its small molecule metabolites. Caffeic acid (3,4-dihydroxycinnamic acid) and its derivatives, including its glycosides and variety of oligomers, which biosynthetically derived from L-phenylalanine and L-tyrosine undergoing a series of enzymatic processes [10,11], are the most common naturally occurring phenolic acids in the plants of family Lamiaceae. In recent years, caffeic acid derivatives from species of family Lamiaceae have been demonstrated to show various bioactivities, such as antiviral, antimicrobial, and antiinflammatory activities, which were believed to be one of the major bioactive components of this plant family [12–17]. However, compared to other species, the investigation about caffeic acid derivatives of *M. chinensis* was insufficient, only about ten caffeic acid derivatives so far have been identified from this plant [18,19].

As part of an ongoing investigation on the discovery of natural products with antiviral activities from medicinal plants growing in southern China [20–22], our preliminary study revealed that the 95% aqueous ethanolic extract of the aerial part of this plant showed promising antiviral activity against respiratory syncytial virus (RSV) with an IC<sub>50</sub> value of 55.00 ± 2.50 µg/µL. The ethanol extract was further partitioned to afford petroleum ether, *n*-BuOH, and water-soluble fractions, respectively. The following bioassay screening indicated that the *n*-BuOH-soluble fraction exhibited the best anti-RSV activity (IC<sub>50</sub> = 13.75 ± 1.45 µg/µL) among the assayed extracts. The HPLC-UV analysis of the *n*-BuOH-soluble fraction showed the characteristic UV profiles that suggested the existence of caffeic acid derivatives as the major components. Based on above results, we carried out a phytochemical investigation on the bioactive fraction of *M. chinensis*. As a result, four new caffeic acid trimers (mesonolates A–D, 1–4) and a new caffeic acid tetramer (mesonolate E, 5), together with four known caffeic acid oligomers, salviaflaside (6), salvianolic acid R (7), lithospermic acid monomethylester (8), and lithospermic acid B (9) (Fig. 1), were isolated from the aforementioned fraction. In addition, all the isolated compounds were evaluated for their *in vitro* anti-RSV activities by cytopathic effect (CPE) reduction assay. Herein, we describe the isolation, structural elucidation, and *in vitro* anti-RSV activities of these caffeic acid oligomers. A hypothetical biogenetic pathway for all the isolated compounds is also discussed.

\* Corresponding authors at: Institute of Traditional Chinese Medicine & Natural Products, College of Pharmacy, Jinan University, Guangzhou 510632, People's Republic of China.

E-mail addresses: [chywc@aliyun.com](mailto:chywc@aliyun.com) (W.-C. Ye), [wangying\\_cpu@163.com](mailto:wangying_cpu@163.com) (Y. Wang).

<sup>1</sup> These authors contributed equally to this work.

<https://doi.org/10.1016/j.fitote.2020.104603>

Received 14 March 2020; Received in revised form 18 April 2020; Accepted 18 April 2020

Available online 28 April 2020

0367-326X/ © 2020 Elsevier B.V. All rights reserved.

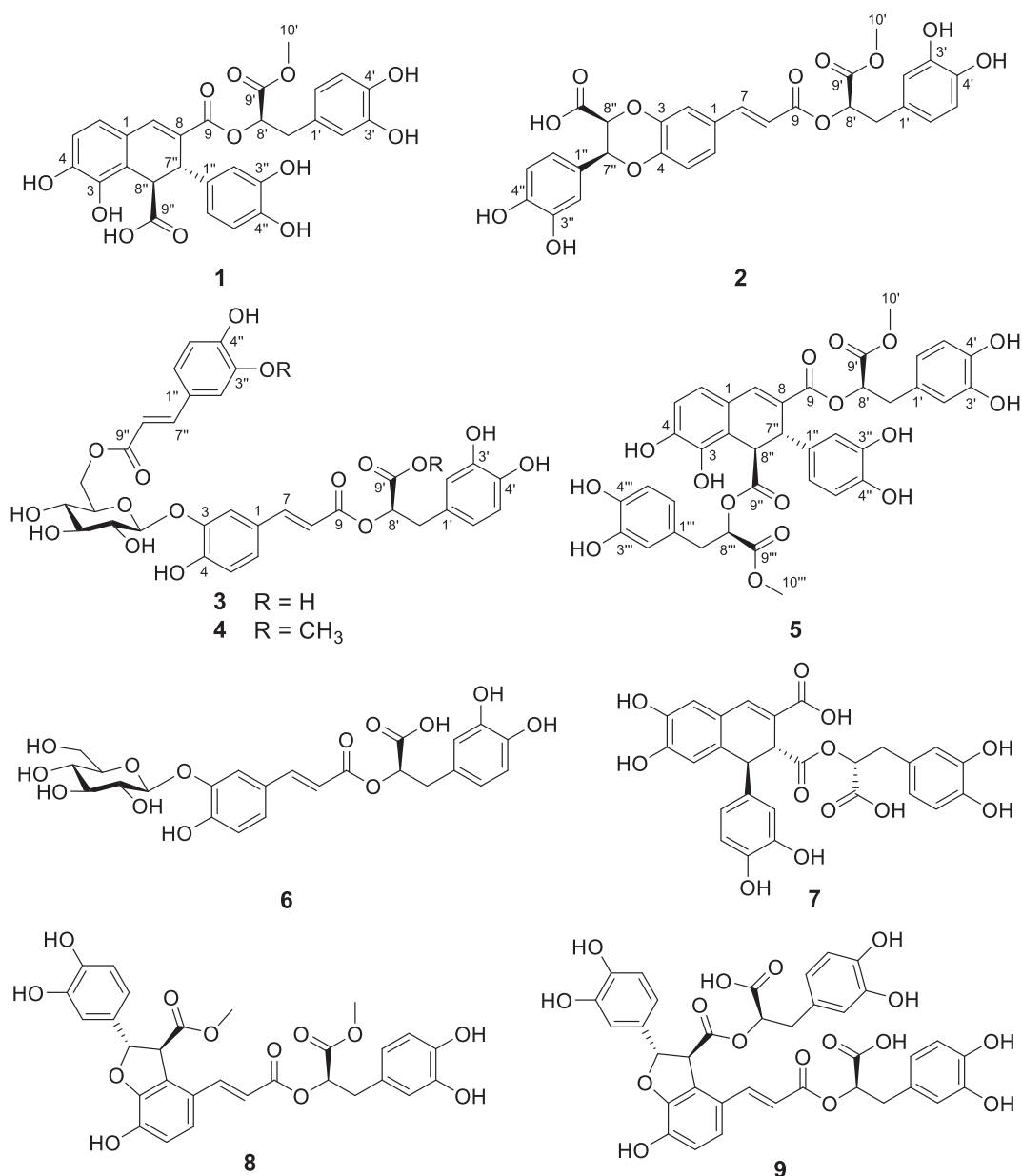


Fig. 1. Chemical structures of compounds 1–9.

## 2. Experimental

### 2.1. General experimental procedures

Optical rotation values were measured on a JASCO P-1020 polarimeter (JASCO, Tokyo, Japan) at room temperature. UV spectra were recorded on a JASCO V-550 UV/vis spectrophotometer. IR spectra were obtained on JASCO FT/IR-480 plus Fourier transform infrared and Nicolet iS50 FT-IR spectrometers using KBr pellets. 1D and 2D NMR spectra, including <sup>1</sup>H, <sup>13</sup>C, DEPT135, <sup>1</sup>H–<sup>1</sup>H COSY, HSQC, HMBC, and NOESY, were collected on Bruker AV-300, Bruker AV-500, and Bruker AV-600 spectrometers. HRESIMS data were collected on an Agilent 6210 ESI/TOF mass spectrometer. ECD spectra were carried out on a Chirascan-plus circular dichroism spectrometer (Applied Photophysics, Leatherhead, Surrey, UK). The pre-coated silica gel GF<sub>254</sub> plate for thin-layer chromatography (TLC) was purchased from the Yantai Chemical Industry Research Institute (Yantai, China). Column chromatographies (CCs) were performed by using silica gel (100–200 and 200–300 mesh, Qingdao Marine Chemical Inc., Qingdao, China), Sephadex LH-20

(Pharmacia Biotech AB, Uppsala, Sweden), and ODS (40–64 μm, Merck, Darmstadt, Germany) as solid phases. Analytical HPLC was performed on an Agilent 1260 liquid chromatograph equipped with a diode array detector (DAD) using a Cosmosil 5C18-MS-II reversed-phase column (4.6 × 250 mm, 5 μm, Nacalai Tesque Inc., Kyoto, Japan). Semi-preparative HPLC was carried on an Agilent 1260 liquid chromatograph equipped with a multiple wavelength detector (MWD) using a semi-preparative Cosmosil 5C18-MS-II reversed-phase column (10 × 250 mm, 5 μm, Nacalai Tesque Inc., Kyoto, Japan). All the solvents used in column chromatographies and HPLC were of analytical grade (Tianjin Damao Chemical Plant, Tianjin, China) and chromatographic grade (Merck, Darmstadt, Germany), respectively.

### 2.2. Plant material

The aerial parts of *Mesona chinensis* Benth. (Lamiaceae) were collected from Pingyuan county of Guangdong province, P. R. China, in July 2018. The authentication of the plant material was performed by Prof. Guang-Xiong Zhou (College of Pharmacy, Jinan University). A

voucher specimen (No. 20180713) was deposited in the Institute of Traditional Chinese Medicine & Natural Products, College of Pharmacy, Jinan University, Guangzhou, P. R. China.

### 2.3. Extraction and isolation

The air-dried and powdered aerial parts (10 kg) of *M. chinensis* were extracted with 95% EtOH (v/v) for four times (4 × 20 L) at room temperature to obtain a crude extract (2 kg), which was then suspended in water and successively partitioned with petroleum ether and *n*-BuOH. The *n*-BuOH-soluble fraction (261.2 g) was separated by silica gel column using chloroform/methanol mixture (100:0 to 0:100, v/v) as eluent to obtain four major fractions (Fr. A–Fr. D). Fr. B (85 g) was subjected to an ODS column and eluted with a gradient mixture of CH<sub>3</sub>CN–H<sub>2</sub>O (20:80 to 100:0, v/v) to afford Fr. Ba–Fr. Bf. Subsequently, Fr. Bc (10.8 g) was chromatographed on a Sephadex LH-20 column (CH<sub>3</sub>OH/H<sub>2</sub>O, 50:50, v/v) to yield three subfractions (Fr. Bc1–Fr. Bc3). Thus, compounds **1** (30 mg) and **5** (10 mg) were isolated from Fr. Bc1 (3 g) by using semi-preparative HPLC (CH<sub>3</sub>CN–H<sub>2</sub>O, 20:80, v/v). Meanwhile, Fr. Bd (20 g) was separated by a Sephadex LH-20 column (CH<sub>3</sub>OH) and followed by repeated preparative HPLC to obtain compounds **6** (58 mg), **8** (60 mg), and **9** (65 mg), respectively. Fr. C (50.5 g) was separated by ODS column using a gradient mixture of CH<sub>3</sub>CN–H<sub>2</sub>O (30:70 to 100:0, v/v) to afford Fr. Ca–Fr. Cd. After that, Fr. Cb (8.2 g) was chromatographed on Sephadex LH-20 column (CH<sub>3</sub>OH/H<sub>2</sub>O, 50:50, v/v) to afford subfractions Fr. Cb1 to Fr. Cb4. Then, Fr. Cb2 (203 mg) was separated by semi-preparative HPLC using CH<sub>3</sub>CN–H<sub>2</sub>O (15:85, v/v) as eluent to afford compounds **2** (36 mg), **3** (12 mg), and **4** (10 mg), respectively. Finally, Fr. Cd (154 mg) was also separated by semi-preparative HPLC (CH<sub>3</sub>OH–H<sub>2</sub>O, 25:75, v/v) to afford compound **7** (51 mg).

#### 2.3.1. Mesonolate A (**1**)

Yellow oil;  $[\alpha]_D^{25} + 61.2$  (c 0.35, CH<sub>3</sub>OH); UV (CH<sub>3</sub>OH)  $\lambda_{\max}$  (log  $\epsilon$ ): 201 (3.96), 288 (3.30), 332 (3.39) nm; IR (KBr)  $\nu_{\max}$  3423, 1697, 1613, 1513, 1450, 1369, 1277, 1169, 1054, 816 cm<sup>-1</sup>; ECD (CH<sub>3</sub>OH,  $\Delta\epsilon$ )  $\lambda_{\max}$  215 (+3.09), 236 (−7.45), 337 (+8.61) nm; <sup>1</sup>H NMR (CD<sub>3</sub>OD, 600 MHz) and <sup>13</sup>C NMR (CD<sub>3</sub>OD, 150 MHz) data, see Table 1; HRESIMS  $m/z$  575.1161 [M + Na]<sup>+</sup> (calcd. for C<sub>28</sub>H<sub>24</sub>O<sub>12</sub>Na: 575.1160).

#### 2.3.2. Mesonolate B (**2**)

Yellow oil;  $[\alpha]_D^{25} + 10.3$  (c 0.35, CH<sub>3</sub>OH); UV (CH<sub>3</sub>OH)  $\lambda_{\max}$  (log  $\epsilon$ ): 202 (3.88), 292 (3.38), 323 (3.29) nm; IR (KBr)  $\nu_{\max}$  3192, 1699, 1607, 1524, 1447, 1366, 1280, 1174, 1117, 1054, 804 cm<sup>-1</sup>; ECD (CH<sub>3</sub>OH,  $\Delta\epsilon$ )  $\lambda_{\max}$  225 (−4.90), 243 (+0.53), 323 (−1.54) nm; <sup>1</sup>H NMR (CD<sub>3</sub>OD, 500 MHz) and <sup>13</sup>C NMR (CD<sub>3</sub>OD, 125 MHz) data, see Table 1; HRESIMS  $m/z$  575.1161 [M + Na]<sup>+</sup> (calcd. for C<sub>28</sub>H<sub>24</sub>O<sub>12</sub>Na, 575.1160).

#### 2.3.3. Mesonolate C (**3**)

Yellow oil;  $[\alpha]_D^{25} - 17.6$  (c 0.35, CH<sub>3</sub>OH); UV (CH<sub>3</sub>OH)  $\lambda_{\max}$  (log  $\epsilon$ ): 199 (3.81), 288 (3.37), 320 (3.41) nm; IR (KBr)  $\nu_{\max}$  3292, 1602, 1522, 1453, 1388, 1269, 1177, 974, 807 cm<sup>-1</sup>; <sup>1</sup>H NMR (CD<sub>3</sub>OD, 600 MHz) and <sup>13</sup>C NMR (CD<sub>3</sub>OD, 75 MHz) data, see Table 1; HRESIMS  $m/z$  707.1583 [M + Na]<sup>+</sup> (calcd. for C<sub>33</sub>H<sub>32</sub>O<sub>16</sub>Na, 707.1583).

#### 2.3.4. Mesonolate D (**4**)

Yellow oil;  $[\alpha]_D^{25} - 27.6$  (c 0.35, CH<sub>3</sub>OH); UV (CH<sub>3</sub>OH)  $\lambda_{\max}$  (log  $\epsilon$ ): 197 (3.71), 292 (2.93), 324 (3.04) nm; IR (KBr)  $\nu_{\max}$  3449, 1688, 1613, 1519, 1453, 1387, 1278, 1177, 1114, 1045, 813 cm<sup>-1</sup>; <sup>1</sup>H NMR (CD<sub>3</sub>OD, 500 MHz) and <sup>13</sup>C NMR (CD<sub>3</sub>OD, 125 MHz) data, see Table 1; HRESIMS  $m/z$  735.1900 [M + Na]<sup>+</sup> (calcd. for C<sub>35</sub>H<sub>36</sub>O<sub>16</sub>Na, 735.1896).

#### 2.3.5. Mesonolate E (**5**)

Yellow oil;  $[\alpha]_D^{25} + 81.1$  (c 0.35, CH<sub>3</sub>OH); UV (CH<sub>3</sub>OH)  $\lambda_{\max}$  (log

$\epsilon$ ): 203 (4.01), 286 (3.40), 337 (3.54) nm; IR (KBr)  $\nu_{\max}$  3286, 1694, 1616, 1516, 1447, 1378, 1272, 1172, 1109, 1051, 813 cm<sup>-1</sup>; ECD (CH<sub>3</sub>OH,  $\Delta\epsilon$ )  $\lambda_{\max}$  217 (+28.56), 240 (−4.98), 331 (+10.03) nm; <sup>1</sup>H NMR (CD<sub>3</sub>OD, 600 MHz) and <sup>13</sup>C NMR (CD<sub>3</sub>OD, 150 MHz) data, see Table 1; HRESIMS  $m/z$  769.1740 [M + Na]<sup>+</sup> (calcd. for C<sub>38</sub>H<sub>34</sub>O<sub>16</sub>Na, 769.1739).

### 2.4. Sugar identification

Samples of compounds **3** and **4** (each 3 mg) were dissolved in 2 mol/L HCl (2 mL) and refluxed at 90 °C for 2 h, respectively. Each solution was evaporated to yield the corresponding residue of each sample. Next, the residues were separately re-dissolved in pyridine (2 mL) and added in L-cysteine methyl ester hydrochloride (3 mg), respectively. The solutions were kept at 60 °C for 1 h, after that, *O*-tolyl isothiocyanate (20  $\mu$ L) was added into each mixture and then heated at 60 °C for another 1 h. Subsequently, HPLC was employed to analyze the reaction mixtures, which was performed on a Cosmosil 5 C18-MS-II column (250 mm × 4.6 mm, 5  $\mu$ m) using CH<sub>3</sub>CN/0.05% HCOOH–H<sub>2</sub>O (25:75, v/v) as the mobile phase. The sugar moieties of **3** and **4** were both determined to be D-glucose by comparison of the retention times of the monosaccharide derivatives ( $t_R$  = 16.48 min) to the derivatives of authentic D-glucose ( $t_R$  = 16.75 min) and L-glucose ( $t_R$  = 15.43 min) [23].

### 2.5. Quantum chemical ECD calculations

The systematic random conformational analyses of the compounds **1**, **2**, and **5** were performed in the SYBYL-X 2.1 program by using MMFF94s molecular force field, which afforded 27, 155, and 26 conformers for compounds **1**, **2**, and **5**, respectively, with an energy cutoff of 10 kcal mol<sup>-1</sup> to the global minima. All the obtained conformers were optimized under B3LYP/6–31+G(d) level in gas phase by using Gaussian09 software [24]. The number of stable conformers (26 for compound **1**, 26 for compound **2**, and 13 for compound **5**, respectively) were subsequently subjected to TDDFT ECD calculations at B3LYP/6–31+G(d) (**1** and **2**) or CAM-B3LYP/6–31+G(d) (**5**) levels, respectively, with the consideration of the first 80 (**1** and **3**) or 50 (**2**) excitations. The overall ECD curves of compounds **1**, **2**, and **5** were all weighted by Boltzmann distribution. Finally, the calculated ECD spectra of compounds **1**, **2**, and **5** were compared with the experimental ones, respectively, by using SpecDis 1.70 software [25].

### 2.6. In vitro anti-RSV assay

Human larynx epidermoid carcinoma cell line (HEp-2, ATCC CCL-23) and respiratory syncytial virus (RSV A2, ATCC VR-1540) were obtained from Medicinal Virology Institute of Wuhan University, China. HEp-2 cells were grown in the growth medium comprising Dulbecco's modified Eagle medium (DMEM, Gibco, USA) supplemented with 10% fetal bovine serum (FBS, Biological Industries) and 1% penicillin-streptomycin. Anti-RSV activities of the compounds (**1–9**) were determined by the cytopathic effect (CPE) reduction assay. HEp-2 cells were seeded in 96-well culture plates (1.5 × 10<sup>4</sup> cells per well) and incubated overnight at 37 °C, 5% CO<sub>2</sub>. The cells were then infected with 100TCID<sub>50</sub> of RSV and treated with various concentrations of compounds (**1–9**) or ribavirin. The RSV-induced CPE was observed and scored at 60 h post-infection. The concentration required to inhibit 50% CPE (IC<sub>50</sub>) was calculated [26]. MTT assay was used to measure the cytotoxicity of the compounds (**1–9**) on HEp-2 cells as described previously [27].

## 3. Results and discussion

Compound **1** was obtained as yellow oil. The HRESIMS of **1** displayed a sodiated molecular ion peak at  $m/z$  575.1161 [M + Na]<sup>+</sup>

**Table 1**  
 $^1\text{H}$  and  $^{13}\text{C}$  NMR spectral data of compounds **1–4** in  $\text{CD}_3\text{OD}$  ( $\delta$  in ppm;  $J$  in Hz).

No.	1		2		3		4	
	$\delta_{\text{H}}$	$\delta_{\text{C}}$	$\delta_{\text{H}}$	$\delta_{\text{C}}$	$\delta_{\text{H}}$	$\delta_{\text{C}}$	$\delta_{\text{H}}$	$\delta_{\text{C}}$
1		126.0		129.6		127.7 <sup>a</sup>		127.6 <sup>a</sup>
2		120.7	7.18 d (2.0)	118.0	7.40 d (2.0)	117.5 <sup>b</sup>	7.42 d (2.0)	117.5 <sup>b</sup>
3		145.2 <sup>a</sup>		146.0 <sup>a</sup>		146.7		146.8 <sup>c</sup>
4		149.5		144.5		151.2		151.3
5	6.74 d (8.2)	114.8	6.96 d (8.4)	118.4	6.86 d (8.4)	117.7 <sup>c</sup>	6.87 d (8.3)	117.6 <sup>b</sup>
6	6.83 d (8.2)	122.6	7.13 dd (8.4, 2.0)	123.7	7.15 dd (8.4, 2.0)	126.4	7.14 dd (8.3, 2.0)	126.5
7	7.70 s	139.9	7.58 d (16.0)	146.8 <sup>b</sup>	7.55 d (15.9)	147.1	7.55 d (16.0)	147.3
8		126.4	6.37 d (16.0)	116.2 <sup>c</sup>	6.35 d (15.9)	115.2 <sup>d</sup>	6.34 d (16.0)	115.1 <sup>d</sup>
9		168.0		167.9		168.2		168.0
1'		128.8		128.5 <sup>d</sup>		129.0		128.6
2'	6.66 d (2.4)	117.4	6.72 d (2.0)	117.5	6.74 d (2.2)	117.4 <sup>c</sup>	6.67 d (2.0)	117.3 <sup>b</sup>
3'		146.1 <sup>b</sup>		146.1 <sup>a</sup>		146.6 <sup>c</sup>		146.2 <sup>c</sup>
4'		145.1 <sup>a</sup>		145.3		145.2		145.4
5'	6.64 d (8.1)	116.4 <sup>c</sup>	6.70 d (8.0)	116.2	6.68 d (8.0)	116.3 <sup>b</sup>	6.67 d (8.0)	116.3 <sup>c</sup>
6'	6.41 dd (8.1, 2.4)	122.0	6.57 dd (8.0, 2.0)	121.8	6.58 dd (8.0, 2.2)	122.0	6.52 dd (8.0, 2.0)	121.9
7'	a 2.98 m b 2.97 m	37.9	a 3.05 dd, (14.2, 5.1) b 3.00 dd, (14.2, 7.6)	38.7	a 3.01 m b 2.94 m	37.8	a 2.92 m b 2.93 m	37.9
8'	5.10 dd (7.0, 5.6)	74.9	5.20 dd (7.6, 5.1)	74.7	5.09 m	74.7	5.01 m	74.7
9'		172.1		172.0		173.4		172.0
10'	3.61 s	52.6	3.69 s	52.7			3.66 s	52.6
1''		134.6		128.7 <sup>d</sup>		127.7 <sup>a</sup>		127.6 <sup>a</sup>
2''	6.53 d (2.5)	115.4	6.86 d (2.0)	115.4	6.91 d (2.0)	115.7 <sup>d</sup>	7.01 d (1.9)	112.1
3''		146.0 <sup>b</sup>		146.4 <sup>b</sup>		149.5		149.2
4''		145.3 <sup>a</sup>		147.0		146.1 <sup>c</sup>		150.6
5''	6.58 d (8.3)	116.3 <sup>c</sup>	6.75 overlapped	116.3 <sup>c</sup>	6.74 d (8.2)	116.5 <sup>c</sup>	6.77 d (8.2)	116.5 <sup>c</sup>
6''	6.47 dd (8.3, 2.5)	119.8	6.75 overlapped	120.1	6.80 dd (8.2, 2.0)	122.7	6.92 dd (8.2, 1.9)	124.0
7''	4.50 d (1.5)	41.9	5.17 d (5.2)	77.0	7.49 d (15.9)	147.4	7.55 d (16.0)	147.3
8''	4.25 d (1.5)	47.4	4.85 d (5.2)	77.6	6.20 d (15.9)	114.8	6.28 d (16.0)	115.1 <sup>d</sup>
9''		176.3		170.8		169.2		169.1
10''							3.84 s	56.5
Glc-1					4.90 d (7.4)	103.3	4.92 d (7.7)	103.2
Glc-2					3.55 m	74.7	3.56 m	74.8
Glc-3					3.55 m	77.4	3.56 m	77.4
Glc-4					3.44 m	72.0	3.42 m	72.2
Glc-5					3.83 ddd (9.4, 6.9, 2.3)	75.6	3.83 m	75.6
Glc-6					4.60 dd (12.0, 2.3) 4.38 dd (12.0, 6.9)	64.7	4.65 dd (11.9, 2.3) 4.35 dd (12.0, 7.5)	65.0

<sup>a–e</sup> Assignments may be interchanged.

(calcd. for  $\text{C}_{28}\text{H}_{24}\text{O}_{12}\text{Na}$ : 575.1160), corresponding to a molecular formula  $\text{C}_{28}\text{H}_{24}\text{O}_{12}$ . The UV spectrum of **1** exhibited characteristic absorptions of caffeic acid derivatives at 201, 288, and 332 nm. The IR spectrum suggested the presence of hydroxy ( $3423\text{ cm}^{-1}$ ), carbonyl ( $1697\text{ cm}^{-1}$ ), and aromatic moieties ( $1613$  and  $1513\text{ cm}^{-1}$ ) in **1**. The  $^1\text{H}$  and  $^{13}\text{C}$  NMR spectra of **1** revealed signals corresponding to three carbonyls ( $\delta_{\text{C}}$  176.3, 172.1, and 168.0), a 1,2,3,4-tetrasubstituted aromatic ring [ $\delta_{\text{H}}$  6.83 (1H, d,  $J = 8.0$  Hz) and 6.74 (1H, d,  $J = 8.0$  Hz);  $\delta_{\text{C}}$  149.5, 145.2, 126.0, 122.6, 120.7, and 114.8], two 1,3,4-trisubstituted aromatic rings [ $\delta_{\text{H}}$  6.66 (1H, d,  $J = 2.4$  Hz), 6.64 (1H, d,  $J = 8.1$  Hz), 6.58 (1H, d,  $J = 8.3$  Hz), 6.53 (1H, d,  $J = 2.5$  Hz), 6.47 (1H, dd,  $J = 8.3, 2.5$  Hz), and 6.41 (1H, dd,  $J = 8.1, 2.4$  Hz);  $\delta_{\text{C}}$  146.1, 146.0, 145.3, 145.1, 134.6, 128.8, 122.0, 119.8, 117.4, 116.4, 116.3, and 115.4], a trisubstituted double bond [ $\delta_{\text{H}}$  7.70 (1H, s);  $\delta_{\text{C}}$  140.0 and 126.4], three methines [ $\delta_{\text{H}}$  5.10 (1H, dd,  $J = 7.0, 5.6$  Hz), 4.50 (1H, d,  $J = 1.5$  Hz), and 4.25 (1H, d,  $J = 1.5$  Hz);  $\delta_{\text{C}}$  75.0, 47.4, and 41.9], a methoxy group [ $\delta_{\text{H}}$  3.61 (3H, s);  $\delta_{\text{C}}$  52.6], and a methylene [ $\delta_{\text{H}}$  2.98 (1H, m) and 2.97 (1H, m);  $\delta_{\text{C}}$  37.9]. The above spectroscopic data together with the molecular formula information suggested that **1** was a caffeic acid trimer with an additional ring in its structure. Based on comprehensive analysis of  $^1\text{H}$ - $^1\text{H}$  COSY, HSQC, and HMBC spectra, the  $^1\text{H}$  and  $^{13}\text{C}$  NMR spectral data of **1** were fully assigned and shown in Table 1.

The  $^1\text{H}$ - $^1\text{H}$  COSY spectrum of **1** revealed the existence of four spin-coupling systems as shown in Fig. 2. In the HMBC spectrum of **1**, correlations between H-6 and C-2/C-4, between H-7 and C-6/C-9, between H-7'/H<sub>3</sub>-10' and C-9', as well as between H-8' and C-1'/C-9 resulted in

the establishment of a methyl rosmarinate motif (**1a**). This assignment was further confirmed by comparing the NMR data assigned for **1a** with those reported in the literature [28]. Meanwhile, the HMBC correlations between H-2'' and C-7'', between H-7'' and C-9'', and between H-8'' and C-1'' allowed the determination of a dihydrocaffeic acid moiety (**1b**). In addition, the HMBC cross-peaks between H-7'' and C-2/C-9 as well as between H-8'' and C-1/C-8 indicated that the above two substructures **1a** and **1b** were coupled through C-2-C-8'' and C-8-C-7'' bonds to form a 1,3-cyclohexadiene ring. Thus, the planar structure of **1** was elucidated as shown in Fig. 2.

Based on the observed NOE correlations between H-8'' and H-2''/H-6'' in the NOESY spectrum of **1**, as well as the characteristic coupling constant of H-7'' and H-8'' ( $J = 1.5$  Hz) [29], a *trans* relationship between H-8'' and H-7'' was established (Fig. 3). Subsequently, the absolute configuration of **1** was determined on the basis of biogenetic perspective and quantum-chemical electronic circular dichroism (ECD) calculation. Structurally, compound **1** possessed a methyl rosmarinate moiety, which was believed to derive from caffeic acid and L-tyrosine undergoing an enzymatic biosynthetic process. Up to now, all reported rosmarinic acid derivatives had a *R* configuration at C-8 position [30,31]. Accordingly, the absolute configuration at C-8' in **1** was deduced as 8'*R*. To determine the absolute configurations of the remaining two stereogenic centers C-7'' and C-8'', two possible absolute structures of **1**, 8'*R*,7''*R*,8''*S*-**1** and 8'*R*,7''*S*,8''*R*-**1**, were subjected to ECD calculations by using Gaussian 09 software, respectively. As shown in Fig. 4, the calculated ECD curve of 8'*R*,7''*S*,8''*R*-**1** showed a good agreement with the experimental one, which was also in accordance

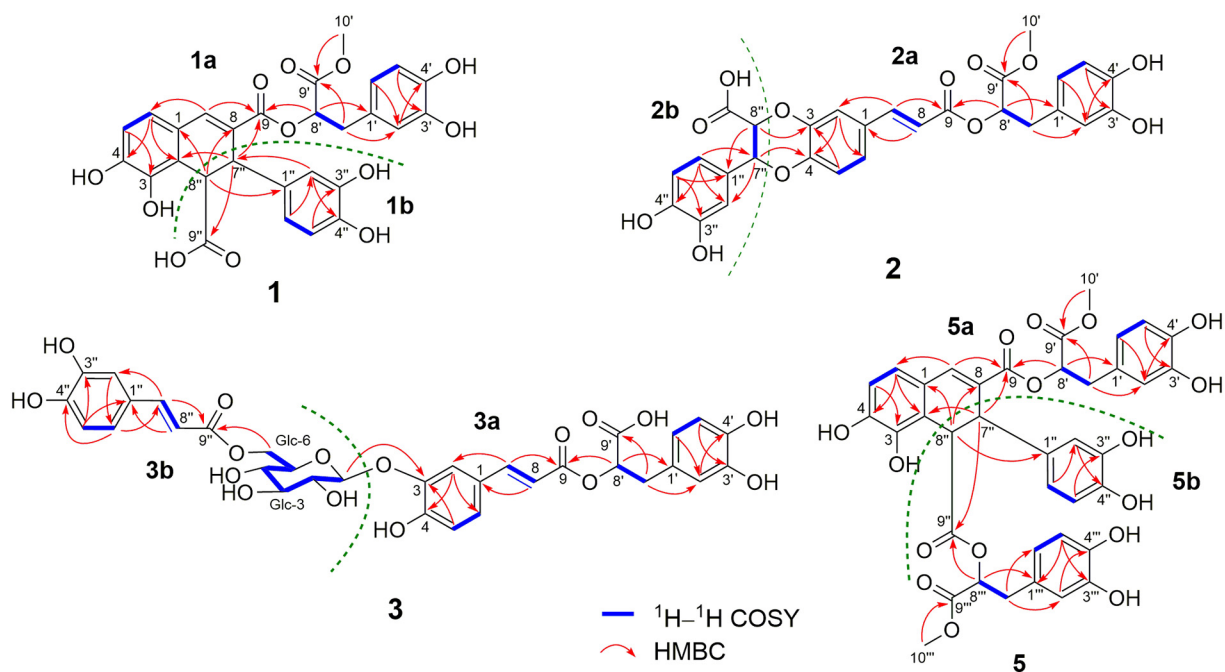


Fig. 2. Key  $^1\text{H}$ - $^1\text{H}$  COSY and HMBC correlations of 1-3 and 5.

with the caffeic acid derivatives with  $7''S,8''R$  configurations reported in the literature [32]. Therefore, the absolute configuration of **1** was confidently established as  $8'R,7''S,8''R$ .

The molecular formula of **2** was determined to be  $\text{C}_{28}\text{H}_{24}\text{O}_{12}$  by its HRESIMS data at  $m/z$  575.1161  $[\text{M} + \text{Na}]^+$  (calcd. for  $\text{C}_{28}\text{H}_{24}\text{O}_{12}\text{Na}$ : 575.1160). Similar to **1**, the UV and IR spectra of **2** showed the typical absorption bands for caffeic acid derivatives. The  $^1\text{H}$  and  $^{13}\text{C}$  NMR spectra of **2** revealed signals for three carbonyls ( $\delta_{\text{C}}$  172.0, 170.8, and 167.9), three 1,3,4-trisubstituted aromatic rings [ $\delta_{\text{H}}$  7.18 (1H, d,  $J = 2.0$  Hz), 7.13 (1H, dd,  $J = 8.4, 2.0$  Hz), 6.96 (1H, d,  $J = 8.4$  Hz), 6.86 (1H, br s), 6.75 (2H, overlapped), 6.72 (1H, d,  $J = 2.0$  Hz), 6.70 (1H, d,  $J = 8.0$  Hz), and 6.57 (1H, dd,  $J = 8.0, 2.0$  Hz);  $\delta_{\text{C}}$  147.0, 146.4, 146.1, 146.0, 145.3, 144.5, 129.6, 128.7, 128.5, 123.7, 121.8, 120.1, 118.4, 118.0, 117.5, 116.3, 116.2, and 115.4], a *trans*-disubstituted double bond [ $\delta_{\text{H}}$  7.58 (1H, d,  $J = 16.0$  Hz) and 6.37 (1H, d,  $J = 16.0$  Hz);  $\delta_{\text{C}}$  146.8 and 116.2], three oxygenated methines [ $\delta_{\text{H}}$  5.20 (1H, dd,  $J = 7.6, 5.1$  Hz), 5.17 (1H, d,  $J = 5.2$  Hz), and 4.85 (1H, d,

$J = 5.2$  Hz);  $\delta_{\text{C}}$  77.6, 77.0, and 74.7], a methoxy group [ $\delta_{\text{H}}$  3.69 (3H, s);  $\delta_{\text{C}}$  52.7], and a methylene [ $\delta_{\text{H}}$  3.05 (1H, dd,  $J = 14.2, 5.1$  Hz) and 3.00 (1H, dd,  $J = 14.2, 7.6$  Hz);  $\delta_{\text{C}}$  38.7]. The above spectroscopic data indicated that **2** was also a caffeic acid trimer. All proton and carbon resonances of **2** were assigned with the assistance of its 1D and 2D NMR spectra (Table 1).

Similar to **1**, compound **2** showed characteristic  $^1\text{H}$  and  $^{13}\text{C}$  NMR signals due to a methyl rosmarinate moiety (**2a**) and a dihydrocaffeic acid unit (**2b**). The existence of substructures **2a** and **2b** were further confirmed by the  $^1\text{H}$ - $^1\text{H}$  COSY and HMBC correlations showed in Fig. 2. Different from **1**, the significant upfield shift at C-8 ( $\delta_{\text{C}}$  116.2) and downfield shifts at C-7'' ( $\delta_{\text{C}}$  77.0) and C-8'' ( $\delta_{\text{C}}$  77.6) were observed in the  $^{13}\text{C}$  NMR spectrum of **2**, suggesting a different coupling pattern between the methyl rosmarinate and dihydrocaffeic acid motifs in **2**. Furthermore, in the HMBC spectrum, cross peaks between H-7'' and C-4 as well as between H-8'' and C-3 were observed, allowing the construction of a benzodioxane ring between fragments **2a** and **2b** via C-

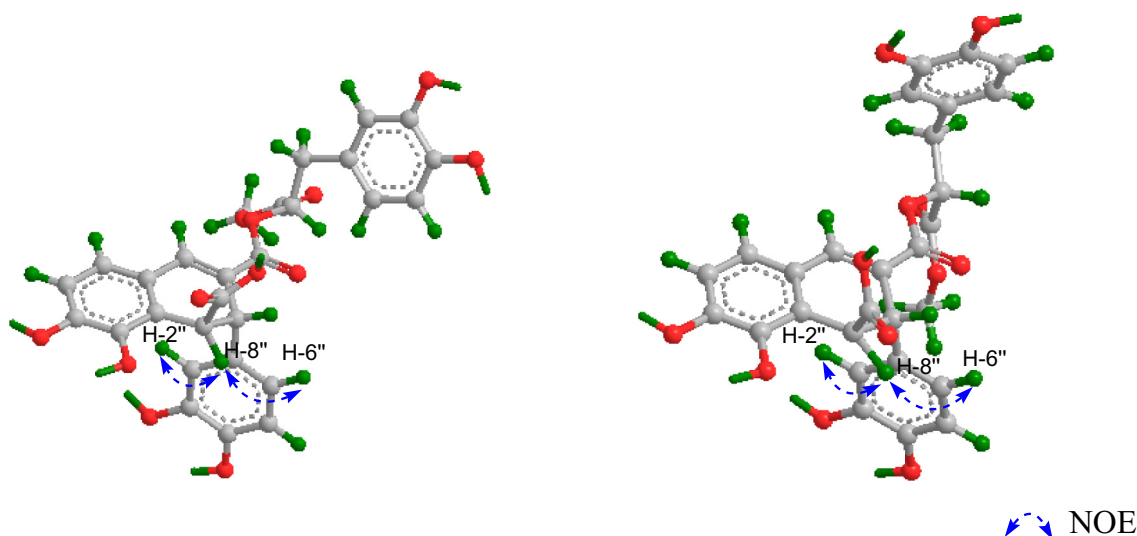


Fig. 3. Key NOE correlations of 1 and 5.

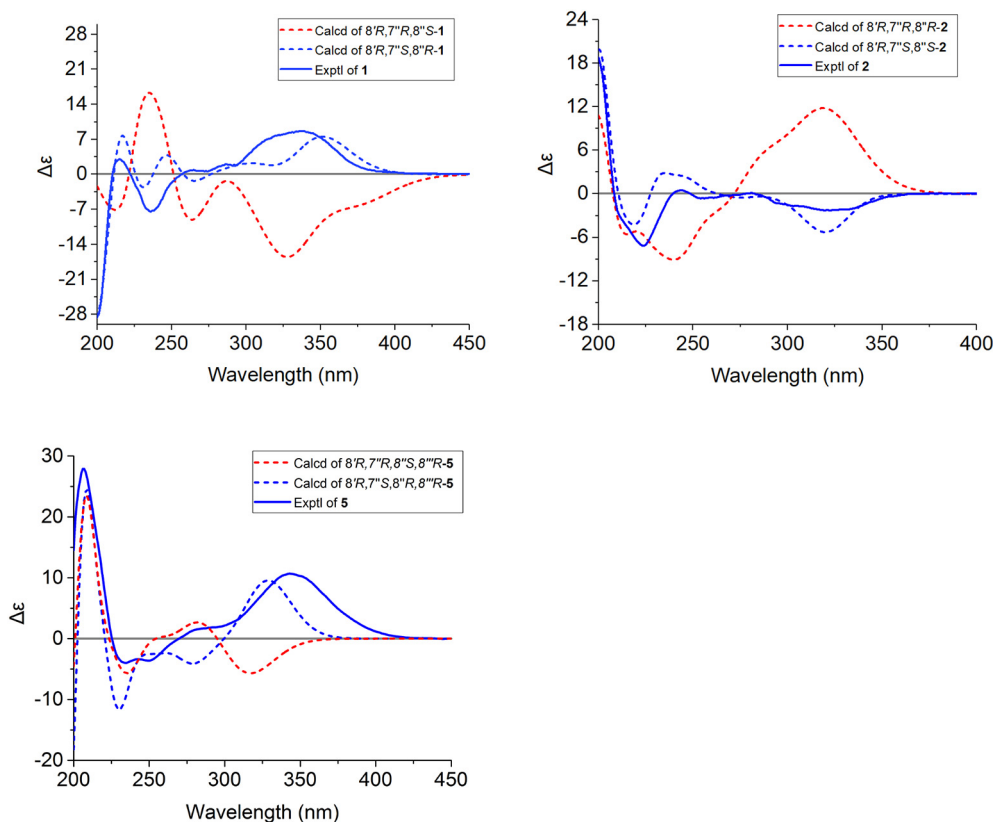


Fig. 4. Experimental and calculated ECD spectra of **1**, **2**, and **5**.

3-O-C-8'' and C-4-O-C-7'' bonds (Fig. 2).

The observed NOE correlation between H-7'' and H-8'' in the NOESY spectrum of **2**, together with the coupling constant of  $^3J_{H-7'',H-8''}$ , indicated the *cis* relationship of H-7'' and H-8'' (Table 1) [33]. Similar to **1**, the absolute configuration of **2** was deduced to be 8'R,7''S,8''S on the basis of biosynthetic consideration and quantum chemical ECD calculation (Fig. 4).

The molecular formula of **3** was assigned as  $C_{33}H_{32}O_{16}$  based on its HRESIMS data at  $m/z$  707.1583  $[M + Na]^+$  (calcd. for  $C_{33}H_{32}O_{16}Na$ : 707.1583). Similar to **2**, the  $^1H$  and  $^{13}C$  NMR spectra of **3** displayed the feature signals of caffeic acid derivatives. In addition, the NMR spectra of **3** showed the signals due to a rosmarinic acid unit instead of the methyl rosmarinate unit in **2**. Besides, the 1D NMR spectra of **3** revealed characteristic signals corresponding to a carbonyl ( $\delta_C$  169.2), a 1,3,4-trisubstituted aromatic ring [ $\delta_H$  6.91 (1H, d,  $J = 2.0$  Hz), 6.80 (1H, dd,  $J = 8.2, 2.0$  Hz), and 6.74 (1H, d,  $J = 8.2$  Hz);  $\delta_C$  149.5, 146.1, 127.7, 122.7, 116.5, and 115.7], a disubstituted double bond [ $\delta_H$  7.49 (1H, d,  $J = 15.9$  Hz) and 6.20 (1H, d,  $J = 15.9$  Hz);  $\delta_C$  147.4 and 114.8], and a sugar moiety [ $\delta_H$  4.90 (1H, d,  $J = 7.4$  Hz), 4.60 (1H, dd,  $J = 12.0, 2.3$  Hz), 4.38 (1H, dd,  $J = 12.0, 6.9$  Hz), 3.83 (1H, ddd,  $J = 9.4, 6.9, 2.3$  Hz), 3.55 (2H, m), 3.44 (1H, m);  $\delta_C$  103.3, 77.4, 75.6, 74.7, 72.0, and 64.7]. After acid hydrolysis of **3**, the obtained monosaccharide derivative was analyzed by HPLC, which resulted in the identification of the sugar unit to be  $D$ -glucose. The  $\beta$ -configuration of the  $D$ -glucose moiety was subsequently determined on the basis of coupling constant of the anomeric proton. The above spectroscopic data and molecular formula information indicated that **3** was a caffeic acid trimer with a  $\beta$ - $D$ -glucose moiety. Comprehensive 1D and 2D NMR spectral data interpretation led to the full assignment of all proton and carbon resonances of **3** (Table 1).

In the  $^1H$ - $^1H$  COSY spectrum of **3**, seven spin-coupling systems could be deduced as shown in Fig. 2. The existence of a rosmarinic acid unit (**3a**) in **3** was verified by the HMBC cross-peaks between H-7 and

C-2/C-9, between H-8 and C-1, between H-7' and C-2'/C-9', as well as between H-8' and C-9/C-1'. Meanwhile, the HMBC correlations between H-2'' and C-6'', between H-5'' and C-1''/C-3'', between H-6'' and C-4'', between H-8'' and C-1'', as well as between H-7'' and C-2''/C-9'' allowed the establishment of a caffeoyl moiety. In the HMBC spectrum, the correlation between H-6 of glucose and C-9' of the caffeoyl moiety was observed, indicating that the caffeoyl moiety was attached to the C-6 position of glucose moiety to form a substructure **3b**. Furthermore, based on the HMBC cross peak between H-1 of the glucose moiety and C-3 of the rosmarinic acid moiety, the fragment **3b** was determined to attach to the C-3 position of fragment **3a** (Fig. 2). The absolute configuration of C-8' was also assigned to be *R* by similar biosynthetic consideration. Therefore, the structure of **3** was determined and shown in Fig. 1.

The molecular formula of **4** was deduced to be  $C_{35}H_{36}O_{16}$  by its HRESIMS at  $m/z$  735.1900  $[M + Na]^+$  (calcd. for  $C_{35}H_{36}O_{16}Na$ : 735.1896), which was 28 mass unit more than that of **3**. The 1D NMR spectra of **4** highly resembled those of **3** (Table 2), with major difference attributed to the presence of  $^1H$  and  $^{13}C$  NMR signals corresponding to two additional methoxyl groups [ $\delta_H$  3.84 (3H, s) and 3.66 (3H, s);  $\delta_C$  56.5 and 52.6] in **4**. In the HMBC spectrum, the correlations between H<sub>3</sub>-10' and C-9' and between H<sub>3</sub>-10'' and C-3'' were observed, indicating that the two additional methoxyl groups were located at C-9' position of the rosmarinic acid moiety and C-3'' position of the caffeoyl moiety, respectively. The sugar unit in **4** was also established as  $\beta$ - $D$ -glucopyranosyl by using the same method as that for **3**. Thus, the structure of **4** was established (Fig. 1).

The molecular formula of **5** was established as  $C_{38}H_{34}O_{16}$  on the basis of its HRESIMS data ( $m/z$  769.1740  $[M + Na]^+$ ; calcd. for  $C_{38}H_{34}O_{16}Na$ : 769.1739). The UV spectrum showed the absorptions maxima at 203, 286, and 337 nm. The IR spectrum exhibited the characteristic absorption bands for hydroxyl ( $3286\text{ cm}^{-1}$ ), carbonyl ( $1694\text{ cm}^{-1}$ ), and benzene ring ( $1616$  and  $1516\text{ cm}^{-1}$ ). The 1D NMR

**Table 2**  
<sup>1</sup>H and <sup>13</sup>C NMR spectral data of compound **5** in CD<sub>3</sub>OD ( $\delta$  in ppm; *J* in Hz).

No.	$\delta_{\text{H}}$	$\delta_{\text{C}}$	No.	$\delta_{\text{H}}$	$\delta_{\text{C}}$
1		126.2	1''		134.1
2		119.6	2''	6.52 d (2.2)	115.4
3		145.2 <sup>a</sup>	3''		145.9 <sup>a</sup>
4		149.5	4''		145.1 <sup>d</sup>
5	6.79 d (8.1)	114.9	5''	6.59 d (8.2)	116.4 <sup>c</sup>
6	6.86 d (8.1)	122.6	6''	6.47 dd (8.2, 2.2)	119.9
7	7.71 s	140.1	7''	4.44 d (1.2)	41.9
8	6.34 d (16.0)	126.2	8''	4.30 d (1.2)	47.5
9		167.9	9''		173.8
1'		128.8 <sup>b</sup>	1'''		128.6 <sup>b</sup>
2'	6.66 d (2.1)	117.4 <sup>c</sup>	2'''	6.54 d (2.1)	117.4 <sup>c</sup>
3'		146.1 <sup>a</sup>	3'''		145.9 <sup>a</sup>
4'		145.1 <sup>a</sup>	4'''		145.3 <sup>d</sup>
5'	6.62 d (8.1)	116.3 <sup>c</sup>	5'''	6.63 d (8.2)	116.3 <sup>c</sup>
6'	6.41 dd (8.1, 2.1)	122.0	6'''	6.30 dd (8.2, 2.1)	122.3
7'	a 2.99 m b 2.98 m	37.9	7'''	a 2.87 dd (14.3, 4.5) b 2.81 dd (14.3, 7.8)	37.6
8'	5.11 dd (7.3, 5.1)	75.0	8'''	4.98 dd (7.8, 4.5)	75.5
9'		172.1	9'''		171.5
10'	3.61 s	52.6	10'''	3.51 s	52.6

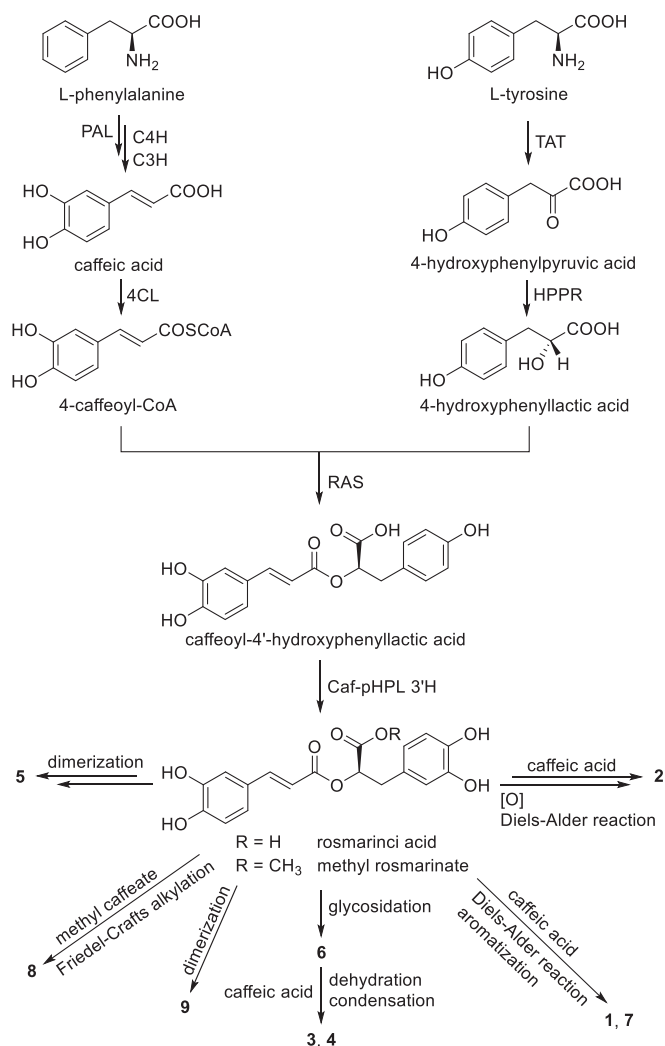
<sup>a-c</sup>Assignments may be interchanged.

spectra of **5** revealed the presence of four carbonyls ( $\delta_{\text{C}}$  173.8, 172.1, 171.5, and 167.9), a 1,2,3,4-tetrasubstituted aromatic ring [ $\delta_{\text{H}}$  6.86 (1H, d, *J* = 8.0 Hz) and 6.79 (1H, d, *J* = 8.0 Hz);  $\delta_{\text{C}}$  149.5, 145.2, 126.2, 122.6, 119.6, and 114.9], three 1,3,4-trisubstituted benzene rings [ $\delta_{\text{H}}$  6.66 (1H, d, *J* = 2.1 Hz), 6.63 (1H, d, *J* = 8.1 Hz), 6.62 (1H, d, *J* = 8.2 Hz), 6.59 (1H, d, *J* = 8.2 Hz), 6.54 (1H, d, *J* = 2.1 Hz), 6.52 (1H, d, *J* = 2.2 Hz), 6.47 (1H, dd, *J* = 8.2, 2.2 Hz), 6.41 (1H, dd, *J* = 8.1, 2.1 Hz), and 6.30 (1H, dd, *J* = 8.2, 2.1 Hz);  $\delta_{\text{C}}$  146.1, 145.9, 145.9, 145.3, 145.1, 145.1, 134.1, 128.8, 128.6, 122.3, 119.9, 120.0, 117.4, 117.4, 116.4, 116.3, 116.3, and 115.4], a trisubstituted double bond [ $\delta_{\text{H}}$  7.71 (1H, s);  $\delta_{\text{C}}$  140.1 and 126.2], four methines [ $\delta_{\text{H}}$  5.11 (1H, dd, *J* = 7.3, 5.1 Hz), 4.98 (1H, dd, *J* = 7.8, 4.5 Hz), 4.44 (1H, d, *J* = 1.2 Hz), and 4.30 (1H, d, *J* = 1.2 Hz);  $\delta_{\text{C}}$  75.5, 75.0, 47.5, and 41.9], two methoxy groups [ $\delta_{\text{H}}$  3.61 (3H, s) and 3.51 (3H, s);  $\delta_{\text{C}}$  52.6 and 52.6], and two methylenes [ $\delta_{\text{H}}$  2.98 (1H, m), 2.97 (1H, m), 2.87 (1H, dd, *J* = 14.3, 4.5 Hz), and 2.81 (1H, dd, *J* = 14.3, 7.8 Hz);  $\delta_{\text{C}}$  37.9 and 37.6]. The above spectroscopic data and molecular formula information indicated that **5** was a caffeic acid tetramer. All the <sup>1</sup>H and <sup>13</sup>C NMR signals of **5** were assigned based on its 1D and 2D NMR spectra (Table 2).

The <sup>1</sup>H – <sup>1</sup>H COSY spectrum of **5** displayed the existence of six spin-coupling systems (Fig. 2). In the HMBC spectrum, cross peaks between H-5 and C-3, between H-6 and C-2/C-4, between H-7 and C-6/C-9, between H-8' and C-9'/C-1', between H-7' and C-2'/C-9', between H-2' and C-4', between H-5' and C-3', between H-6' and C-2', as well as between H<sub>3</sub>-10' and C-9' allowed the establishment of a methyl rosmarinate unit (5a) in **5**, which was identical to the fragment **1a** in **1**. In addition, the HMBC correlations between H-5''' and C-1'''/C-3''', between H-7''' and C-2'''/C-6''', between H-8''' and C-1'''/C-9'', between H-7'' and C-9'', between H-8'' and C-1'', between H-5'' and C-3'', between H-2'' and C-4'', as well as between H<sub>3</sub>-10''' and C-9''' led to the construction of a methyl dihydrorosmarinate unit (5b) in **5**. Furthermore, the connection of substructures 5a and 5b through C-2–C-8'' and C-8–C-7'' bonds were respectively deduced by the HMBC cross-peaks between H-7'' and C-2'/C-9 as well as between H-8'' and C-1'/C-8. Thus, the planar structure of **5** was elucidated and shown in Fig. 2.

Similar to **1**, the *trans* relationship between H-7'' and H-8'' was determined by NOE correlations between H-8'' and H-2''/H-6'' in its NOESY spectrum. Subsequently, the absolute configuration of **5** was established to be 8''R,7''S,8''R,8''R employing the same method as described for **1** (Fig. 4).

The structures of the four known compounds **6**–**9** were identified as



**Scheme 1.** Hypothetical biosynthetic pathways for compounds **1**–**9**. The involved enzymes are: PAL = phenylalanine ammonia lyase; C4H = cinnamic acid 4-hydroxylase; C3H = cinnamic acid 3-hydroxylase; 4CL = 4-coumaric acid CoA-ligase; TAT = tyrosine aminotransferase; HPPR = hydroxyphenylpyruvate reductase; RAS = rosmarinic acid synthase; Caf-pHPL 3'H = caffeoyl-4'-hydroxyphenyllactate 3'-hydroxylase.

salviaflaside (**6**) [34], salvianolic acid R (**7**) [35], lithospermic acid monomethylester (**8**) [36], and lithospermic acid B (**9**) [37], respectively, by comparison of their spectral data with the literature values. Compounds **1**–**9** are nine caffeic acid oligomers with different degree and mode of polymerization. A brief hypothetical biogenetic pathway for these compounds was proposed as shown in Scheme 1 [10,11,38,39].

All the isolated compounds (**1**–**9**) were evaluated for their *in vitro* anti-RSV activities using the cytopathic effect (CPE) reduction assay. As a result (Table 3), compounds **7** and **9** exhibited promising anti-RSV activities with IC<sub>50</sub> values of 5.00 ± 1.25 μM and 21.25 ± 0.25 μM, respectively, whereas the anti-RSV activities of compounds **1**, **2**, **5**, and **8**, esterifying at C-9' carboxyl, decreased significantly. Meanwhile, the three caffeic acid glycoside oligomers (**3**, **4**, and **6**) did not show an anti-RSV effect under the higher concentration of 50 μM.

#### 4. Conclusion

The phytochemical investigation on a bioactive fraction of the aerial parts of *M. chinensis* resulted in the discovery of nine caffeic acid oligomers. Among them, mesonolates A–D (**1**–**4**) are four new caffeic acid

**Table 3**  
The *In vitro* anti-RSV activities of compounds 1–9.

Compounds	IC <sub>50</sub> ± SD (μM) <sup>a</sup>	CC <sub>50</sub> ± SD (μM) <sup>b</sup>
1	47.5 ± 2.50	> 50
2	> 50	> 50
3	> 50	> 50
4	> 50	> 50
5	> 50	> 50
6	> 50	> 50
7	5.00 ± 1.25	> 50
8	47.5 ± 2.50	> 50
9	21.25 ± 0.25	> 50
Ribavirin <sup>c</sup>	6.88 ± 0.63	> 50

<sup>a</sup> IC<sub>50</sub> is the concentration of compound that reduced 50% CPE compared to control cells infected with RSV.

<sup>b</sup> CC<sub>50</sub> is the concentration of compound corresponding to half maximal inhibition of the growth and survival of HEP-2 cells.

<sup>c</sup> Ribavirin was used as the positive control.

trimers and mesonolate E (5) is a new caffeic acid tetramer. In addition, compounds 1 and 7–9 displayed *in vitro* anti-RSV activities to a different extent with IC<sub>50</sub> values ranging from 5.00 ± 1.25 μM to 47.5 ± 2.50 μM. Notably, compound 7 showed the strongest anti-RSV activity, which was comparable to that of the positive control ribavirin. This study suggested that caffeic acid derivatives might be the major active components contributed to the anti-RSV activity of *M. chinensis*.

## Acknowledgements

This work was financially supported by the National Mega-Project for Innovative Drugs (2019ZX09735002), the National Key R&D Program of China (2017YFC1703800), the National Natural Science Foundation of China (81630095 and 81622045), and the Local Innovative and Research Teams Project of Guangdong Pearl River Talents Program (2017BT01Y036). This work was also supported by the high-performance computing platform of Jinan University.

## Declaration of Competing Interest

The authors declare that they have no conflicts of interest.

## Appendix A. Supplementary data

Supplementary data to this article can be found online at <https://doi.org/10.1016/j.fitote.2020.104603>.

## References

- [1] Lamiaceae, in: X.W. Li, C.H. Lan, Flora of China (Eds.), Editorial Committee of Flora of China, Science Press, Beijing, 1994, p. 297.
- [2] H.C. Huang, S.H. Chuang, Y.C. Wu, P.M. Chao, Hypolipidaemic function of Hsian-tso tea (*Mesona procumbens* Hems!): working mechanisms and active components, *J. Funct. Foods* 26 (2016) 217–227.
- [3] C.Y. Huang, G.C. Yen, Antioxidant activity of phenolic compounds isolated from *Mesona procumbens* Hems!, *J. Agric. Food Chem.* 50 (2002) 2993–2997.
- [4] T. Feng, Z.B. Gu, Z.Y. Jin, H.N. Zhuang, Isolation and characterization of an acidic polysaccharide from *Mesona Blumes* gum, *Carbohydr. Polym.* 71 (2008) 159–169.
- [5] W.J. Wang, L. Jiang, Y.M. Ren, M.Y. Shen, J.H. Xie, Characterizations and hepatoprotective effect of polysaccharides from *Mesona blumes* against tetrachloride-induced acute liver injury in mice, *Int. J. Biol. Macromol.* 124 (2019) 788–795.
- [6] T. Feng, M. Sang, H.N. Zhuang, Z.M. Xu, *In vitro* and *in vivo* antioxidative and radioprotective capacities of polysaccharide isolated from *Mesona Blumes* gum, *Starch* 69 (2017) 1700056.
- [7] W. Tang, M.Y. Shen, J.H. Xie, D. Liu, M.X. Du, L.H. Lin, H. Gao, B.R. Hamaker, M.Y. Xie, Physicochemical characterization, antioxidant activity of polysaccharides from *Mesona chinensis* Benth and their protective effect on injured NCTC-1469 cells induced by H<sub>2</sub>O<sub>2</sub>, *Carbohydr. Polym.* 175 (2017) 538–546.
- [8] L.X. Huang, M.Y. Shen, P.W. Wen, T. Wen, Y.Z. Hong, Q. Yu, M. Huang, Y. Chen, J.H. Xie, Sulfated modification enhanced the antioxidant activity of *Mesona chinensis* Benth polysaccharide and its protective effect on cellular oxidative stress, *Int. J. Biol. Macromol.* 136 (2019) 1000–1006.

- [9] Y. Anynda, G.K.K. Tha, H.A. Keith, M.M. Lara, The effect of gel structure on the *in vitro* digestibility of wheat starch-*Mesona chinensis* polysaccharide gels, *Food Funct.* 10 (2019) 250–258.
- [10] P. Maike, A. Yana, B. Johannes, E. David, G. Katja, H. Stephanie, J. Verena, H.K. Kyung, S. Marion, W. Corinna, W. Stefan, Evolution of rosmarinic acid biosynthesis, *Phytochemistry* 70 (2009) 1663–1679.
- [11] Y.F. Bao, X.C. Shen, F. Wang, The research progress and development prospects of biosynthesis, structure activity relationship and biological activity of caffeic acid and its main types of derivatives, *Nat. Prod. Res. Dev.* 30 (2018) 1825–1833.
- [12] J.L. Zhang, R.J. Yan, X. Zhang, D.J. Chen, T. Wu, J.G. Xin, A new caffeic acid tetramer from the *Dracocephalum moldavica* L, *Nat. Prod. Res.* 32 (2018) 370–373.
- [13] H.G. Choi, P.T. Tran, J.H. Lee, B.S. Min, J.A. Kim, Anti-inflammatory activity of caffeic acid derivatives isolated from the roots of *Salvia miltiorrhiza* Bunge, *Arch. Pharm. Res.* 41 (2018) 64–70.
- [14] J. Kang, Y. Tang, Q. Liu, N. Guo, J. Zhang, Z. Xiao, R. Chen, Z. Shen, Isolation, modification, and aldose reductase inhibitory activity of rosmarinic acid derivatives from the roots of *Salvia grandifolia*, *Fitoterapia* 112 (2016) 197–204.
- [15] T.J. Ha, J.H. Lee, M.H. Lee, B.W. Lee, H.S. Kwon, C.H. Park, K.B. Shim, H.T. Kim, I.Y. Baek, D.S. Jang, Isolation and identification of phenolic compounds from the seeds of *Perilla frutescens* (L.) and their inhibitory activities against alpha-glucosidase and aldose reductase, *Food Chem.* 135 (2012) 1397–1403.
- [16] Z.C. Sun, Q.X. Zheng, G.X. Ma, J.Q. Yuan, H.F. Wu, H.L. Liu, J.S. Yang, X.D. Xu, Four new phenolic acids from *Clerodendranthus spicatus*, *Phytochem. Lett.* 8 (2014) 16–21.
- [17] M. Toshihiro, W. Mai, T. Yu, M. Toshio, Y. Fumihiko, Hyaluronidase inhibitors from Takuran, *Lycopus lucidus*, *Chem. Pharm. Bull.* 58 (2010) 394–397.
- [18] F. Wang, R.Y. Xiang, C.Z. Lin, C.C. Zhu, Chemical constituents from *Mesona chinensis*, *J. Chin. Med. Mater.* 40 (2017) 2839–2843.
- [19] L.H. Qin, X.Y. Guo, M. Fan, A.S. Ding, N.L. Wang, X.S. Yao, Anti-anoxic constituents from *Mesona chinensis* Benth, *J. Shenyang Pharm. Univ.* 23 (2006) 633–636.
- [20] J. Liu, J.G. Song, J.C. Su, X.J. Huang, W.C. Ye, Y. Wang, Tomentodione E, a new sec-pentyl syncarpic acid-based meroterpenoid from the leaves of *Rhodomyrtus tomentosa*, *J. Asian Nat. Prod. Res.* 20 (2017) 67–74.
- [21] J.C. Su, W. Cheng, J.G. Song, Y.L. Zhong, X.J. Huang, R.W. Jiang, Y.L. Li, M.M. Li, W.C. Ye, Y. Wang, Macrocylic diterpenoids from *Euphorbia helioscopia* and their potential anti-inflammatory activity, *J. Nat. Prod.* 82 (2019) 2818–2827.
- [22] J.G. Song, J.C. Su, Q.Y. Song, R.L. Huang, W. Tang, L.J. Hu, X.J. Huang, R.W. Jiang, Y.L. Li, W.C. Ye, Y. Wang, Cleistocalones A and B, antiviral phloroglucinol–terpenoid adducts from *Cleistocalyx operculatus*, *Org. Lett.* 21 (2019) 9579–9583.
- [23] S.G. Li, X.J. Huang, M.M. Li, Q. Liu, H. Liu, Y. Wang, W.C. Ye, Multiflorumisides A–G, dimeric stilbene glucosides with rare coupling patterns from the roots of *Polygonum multiflorum*, *J. Nat. Prod.* 81 (2018) 254–263.
- [24] M.J. Frisch, G.W. Trucks, H.B. Schlegel, G.E. Scuseria, M.A. Robb, J.R. Cheeseman, G. Scalmani, V. Barone, B. Mennucci, G.A. Petersson, H. Nakatsuji, M. Caricato, X. Li, H.P. Hratchian, A.F. Izmaylov, J. Bloino, G. Zheng, J.L. Sonnenberg, M. Hada, M. Ehara, K. Toyota, R. Fukuda, J. Hasegawa, M. Ishida, T. Nakajima, Y. Honda, O. Kitao, H. Nakai, T. Vreven, J.A. Montgomery Jr., J.E. Peralta, F. Ogliaro, M. Bearpark, J.J. Heyd, E. Brothers, K.N. Kudin, V.N. Staroverov, T. Keith, R. Kobayashi, J. Normand, K. Raghavachari, A. Rendell, J.C. Burant, S.S. Iyengar, J. Tomasi, M. Cossi, N. Rega, J.M. Millam, M. Klene, J.E. Knox, J.B. Cross, V. Bakken, C. Adamo, J. Jaramillo, R. Gomperts, R.E. Stratmann, O. Yazyev, A.J. Austin, R. Cammi, C. Pomelli, J.W. Ochterski, R.L. Martin, K. Morokuma, V.G. Zakrzewski, G.A. Voth, P. Salvador, J.J. Dannenberg, S. Dapprich, A.D. Daniels, O. Farkas, J.B. Foresman, J.V. Ortiz, J. Cioslowski, D.J. Fox, Gaussian 09, Revision D.01, Gaussian, Inc, Wallingford CT, 2013.
- [25] T. Bruhn, A. Schaumloffel, Y. Hemberger, G. Pescitelli, SpecDis version 1.70, Berlin, Germany, (2017).
- [26] W. Tang, M. Li, Y. Liu, N. Liang, Z. Yang, Y. Zhao, S. Wu, S. Lu, Y. Li, F. Liu, Small molecule inhibits respiratory syncytial virus entry and infection by blocking the interaction of the viral fusion protein with the cell membrane, *FASEB J.* 33 (2018) 4287–4299.
- [27] J.J. Xu, Z. Liu, W. Tang, G.C. Wang, H.Y. Chuang, Q.Y. Liu, L. Zhuang, M.M. Li, Y.L. Li, Tangeretin from citrus reticulate inhibits respiratory syncytial virus replication and associated inflammation *in vivo*, *J. Agric. Food Chem.* 63 (2015) 9520–9527.
- [28] H. Huang, Phenolic compounds of *Isodon oresbius*, *J. Nat. Prod.* 59 (1996) 1079–1080.
- [29] I. Agata, T. Hatano, S. Nishibe, T. Okuda, Rabdosiin, a new rosmarinic acid dimer with a lignin skeleton from *Rabosia japonica*, *Chem. Pharm. Bull.* 36 (1988) 3223–3225.
- [30] C.B. Ai, Q.H. Deng, W.Z. Song, L.N. Li, Salvanolic acid J, a depside from *Salvia flava*, *Phytochemistry* 37 (1994) 907–908.
- [31] Q.X. Zheng, Z.C. Sun, X.P. Zhang, J.Q. Yuan, H.F. Wu, J.S. Yang, X.D. Xu, Clerodendranic acid, a new phenolic acid from *Clerodendranthus spicatus*, *Molecules* 17 (2012) 13656–13661.
- [32] N. Makoto, T. Masashi, H. Koji, Two caffeic acid tetramers having enantiomeric phenyldihydronaphthalene moieties from *Macrotomia euchroma*, *Phytochemistry* 29 (1990) 2645–2649.
- [33] T. Murata, K. Sasaki, K. Sato, F. Yoshizaki, H. Yamada, H. Mutoh, K. Umehara, T. Miyase, T. Warashina, H. Aoshima, H. Tabata, K. Matsubara, Matrix metalloproteinase-2 inhibitors from *Clinopodium chinense* var. *parviflorum*, *J. Nat. Prod.* 72 (2009) 1379–1384.
- [34] X.J. Zhou, L.L. Yan, P.P. Yin, L.L. Shi, J.H. Zhang, Y.J. Liu, C. Ma, Structural characterisation and antioxidant activity evaluation of phenolic compounds from cold-pressed *Perilla frutescens* var. *arguta* seed flour, *Food Chem.* (164) (2014)

- 150–157.
- [35] V. Exarchou, P.G. Takis, M. Malouta, J. Vervoort, E. Karali, A.N. Trognis, Four new depsides in *Origanum dictamnus* methanol extract, *Phytochem. Lett.* 6 (2013) 46–52.
- [36] H. Kohda, O. Takeda, S. Tanaka, K. Yamasaki, A. Yamashita, T. Kurokawa, S. Ishibashi, Isolation of inhibitors of adenylate cyclase from dan-shen, the root of *Salvia miltiorrhiza*, *Chem. Pharm. Bull.* 37 (1989) 1287–1290.
- [37] Z.J. Wu, M.A. Ouyang, C.R. Chong, Polyphenolic constituents of *Salvia sonchifolia*, *Acta Bot. Yunnanica* 21 (1999) 393–398.
- [38] D. Peng, L. Zhang, J.F. Chen, H.X. Tan, Y. Xiao, X. Dong, X. Zhou, W.S. Chen, <sup>13</sup>C tracer reveals phenolic acids biosynthesis in hairy root cultures of *Salvia miltiorrhiza*, *ACS Chem. Biol.* 8 (2013) 1537–1548.
- [39] H. Liu, Y. Fu, H. Sun, Y.F. Zhang, X.Z. Lan, Transcriptomic analyses reveal biosynthetic genes related to rosmarinic acid in *Dracocephalum tanguticum*, *Sci. Rep.* 74 (2017) 1–10.